ELSEVIER

Journal of Nuclear Materials 302 (2002) 175–184

journal of nuclear materials

www.elsevier.com/locate/jnucmat

Study of the α/β phase transformation of Zy-4 in presence of applied stresses at heating: analysis of the inherited microstructures and textures

N. Gey [a,*], E. Gautier [b], M. Humbert [a], A. Cerqueira [c], J.L. Bechade [c], P. Archambault [b]

[a] *LETAM-ISGMP UMR 7078, Université de Metz, Ile de Saulcy, F-57045 Metz cedex, France*
[b] *LSG2M UMR 7584, Ecole des Mines, Parc Saurupt, F-54042 Nancy cedex, France*
[c] *CEA Saclay, DEN/SRMA, F-91191 Gif sur Yvette cedex, France*

Received 6 November 2001; accepted 17 January 2002

Abstract

The α → β → α phase transformation of Zy-4, as well as the inherited microstructures and textures have been investigated, in presence (or not) of applied tensile stress during the anisothermal α → β transformation. Without applied stress, the β treatment led to an inherited α texture sharper than the initial one. A detailed analysis of this texture change revealed a strong variant selection in the β → α transformation. With applied stress, transformation plasticity as well as creep of the β phase were clearly identified on the dilatometric curves. Moreover, the sharpness of the inherited α texture was significantly reduced. This has been related to a strong reduction of variant selection in the β → α transformation.

1. Introduction

Zircaloy-4 (Zy-4) is widely used for nuclear applications, in particular as material for fuel cladding tubes of nuclear pressurized water reactors. Under usual working conditions, the temperature of the tube is about 300 °C [1]. However, a loss of coolant accident (LOCA) would rapidly submit the tube to a temperature increase up to 700–1000 °C and consequently to an internal pressure increase [2].

In this temperature range, Zy-4 undergoes the α/β phase transformation. Thus, during a LOCA, the transformation occurs under a stress field leading to a complex mechanical behavior of the tube. Indeed, if the phase transformation occurs under applied stresses, a transformation-induced plasticity is often observed [3–10]. Such a phenomenon was obtained for zirconium [3,4] and Zy-4 alloy [5]. The origin of transformation plasticity deformation is attributed to two basic mechanisms in the case of transformation involving a shear deformation component and a volume variation [6,7]. The first mechanism results from a favorable orientation of the transformed phase in the presence of an applied stress [8] and the second one from the anisotropic plastic accommodation of the transformation deformation associated with the local stress field [3]. Thus, in addition to the change in mechanical behavior, the microstructure and the orientation of the transformation product can be modified.

This contribution reports the influence of an axial applied stress at heating on the α → β → α phase transformation as well as on the inherited microstructures and textures. Different thermo-mechanical tests have been performed in which the transformation at heating occurred with and without a constant applied stress along the axial direction of the samples. The phase transformation evolution has been continuously studied thanks to in situ electrical resistivity measurements. The

* Corresponding author.
E-mail address: gey@letam.sciences.univ-metz.fr (N. Gey).

0022-3115/02/$ - see front matter
PII: S0022-3115(02)00789-4

experiments confirmed the existence of transformation-induced plasticity. The texture modifications induced by the $\alpha \rightarrow \beta \rightarrow \alpha$ phase transformation sequence have been characterized in details. Moreover, the intermediate β texture have been evaluated by adapted restitution methods. Finally, the influence of an axial applied stress at heating on the high temperature β textures and the inherited α textures are discussed.

2. Experimental procedure

2.1. Thermo-mechanical test

All tests have been performed using in-house thermo-mechanical simulators (DITHEM or a quenching dilatometer) allowing to control thermal and mechanical cycles.

The actual sample holder of DITHEM is not suitable for working on tubes. Thus the samples used in this investigation, were taken from the core of a Zy-4 rod as described in Fig. 1(a). Their gage dimensions were 4 mm in diameter and 30 mm in length for the quenching dilatometer samples, and 6 mm in diameter and 30 mm in length for the thermo-mechanical simulator samples. The axial direction (AD) of the different samples is parallel to the AD of the initial rod. Thus, in the following, the abbreviation AD refers to the axial direction of both, the Zy-4 rod and the samples.

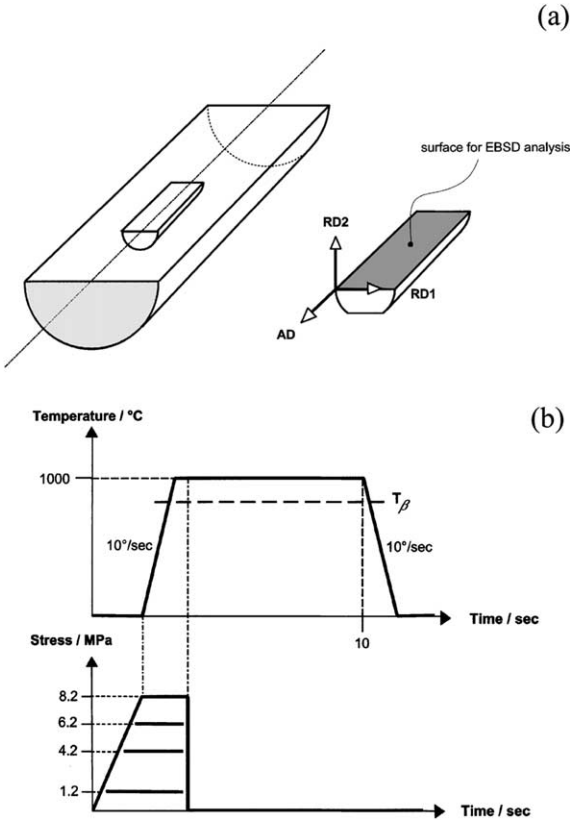

Fig. 1. (a) Schematic representation of a sample and its principal directions (AD, RD_1, RD_2). (b) Thermo-mechanical treatment conditions.

The tests were carried out in secondary vacuum to avoid sample oxydation. The treatment conditions are schematically represented in Fig. 1(b). The sample was heated up to 1000 °C with a rate of 10 °C/s, and maintained 10 s to limit the β grain coarsening. The cooling (10 °C/s) was obtained by helium sprayed on the sample.

A controlled load was imposed by an hydraulic actuator during the heating step and removed after the temperature of 1000 °C was reached and maintained a few seconds. The tensile stresses were applied parallel to AD and the amplitude varied from 0 to 8.2 MPa. The length and electrical resistivity variations of the sample were continuously measured during the treatment in order to characterize respectively the deformation of the material and the progression of the $\alpha \rightarrow \beta \rightarrow \alpha$ phase transformations. The length variations have been measured along AD.

2.2. Texture determination

The textures were determined from a significant number of individual grain orientations deduced from electron back scattered Kikuchi patterns obtained in a scanning electron microscope (SEM) [11]. The pole figure measurement using a texture goniometer was not adapted, because of the coarse α colonies of the inherited microstructure.

The individual orientations have been measured in a longitudinal section of the samples as indicated in Fig. 1(a). Automatic displacement of the specimen holder in the SEM chamber allowed to investigate a large area representative of the sample.

The orientation density functions (ODF) were obtained by superposition of Gaussian functions centered on the measured orientations and equally weighted. Their spreads were fixed to 8° according to the number of grain orientations and the hexagonal crystal symmetry [12]. Practically, each function was developed into a series expansion on the basis of spherical harmonic functions (see Eq. (1)).

In this contribution, the textures are represented by means of characteristic poles figures. The projection plane of the pole figures is perpendicular to AD. Such a representation makes easy the observation of an axi-symmetric orientation distribution around AD.

$$f(g) = \sum_{l=0}^{+\infty} \sum_{m=-1}^{1} \sum_{n=-1}^{1} \boldsymbol{C}_l^{mn} \boldsymbol{T}_l^{mn}(g). \quad (1)$$

3. Experimental result

3.1. Characterization of the as received material

As detailed previously, the dilatometric samples were taken from the core of a Zy-4 rod, 24 mm in diameter. The rod has been extruded in the β field and then in the high temperature range of the α field. At this stage of the industrial transformation process, the material seems to be partially recrystallized. The chemical composition of the rod is given in Table 1. It is homogeneous over the section.

The initial α phase exhibits an equiaxed morphology of grains with an heterogeneous grain size distribution (see Fig. 2). This heterogeneity can be linked to differences in the metallurgical state of the α phase; i.e. differences in the level of deformation, recovery and recrystallization from one grain to the other.

The orientation distribution of the initial material has been determined from a great number of orientations measured in the core of the Zy-4 rod, in a longitudinal section (to be coherent with the orientation measurements performed on the dilatometric samples). The texture of the initial material (see Fig. 3) is nearly symmetric around AD, because of the axi-symmetry of the transformation process. It can be characterized by several $\langle uv.0\rangle//AD$ fibers. As seen in Fig. 3, the $\vec{c}$ axes of the α crystallites are tilted toward the radial directions (RD) of the rod. The crystallographic planes such as {10.0} or {11.0} planes are parallel to the cross section of the rod. Some characteristic values of this texture are summarized in Table 2. The texture index of 2.5 and the ODF maximum of 6 indicate the sharpness of the texture.

This α texture is different from that of a cladding tube. The latter mainly exhibits the $\vec{c}$ axes in the radial–tangential plane, tilted of about 40° from the RD. Such differences in the texture are related to differences in the transformation process between a rod (extrusion) and a tube (cold rolling) [13]. However if we take into account the axial direction of both materials (direction of the applied stress during heating with the DITHEM), the rod and the tube show nearly the same kind of texture (Kearns factors $fA^{tube} \sim 0.1$ and $fA^{rod} \sim 0.09$). Thus, it can be assumed that the results concerning the texture evolution obtained in this study can be transposed to the tube.

Table 1
Chemical composition of the Zy-4 rod (wt%)

Sn (%)	Fe (%)	Cr (%)	Oxygen (ppm)
1.46	0.23	0.10	1150

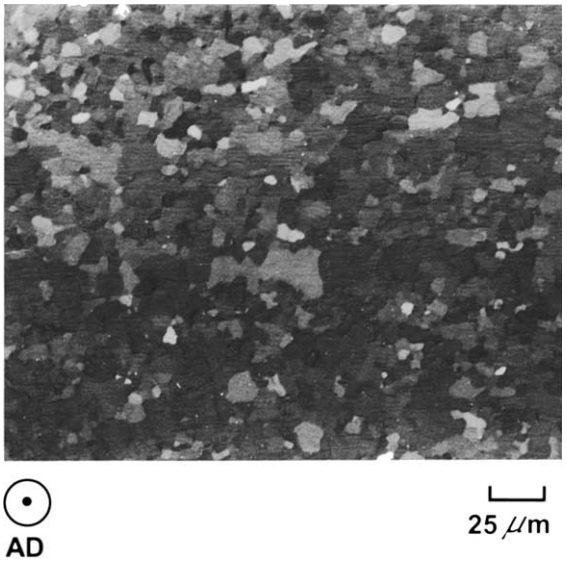

Fig. 2. Microstructure of the initial α phase.

3.2. Material behavior for transformation without applied stress

3.2.1. Length and electrical resistivity variations

The length and normalized electrical resistance variations during heating are reported in Fig. 4 for no applied stress. These length variations correspond to measurements along AD.

The transformation temperature range during heating can thus be determined by both measurements. Dilatometric measurements indicate that the transformation starts at 850 °C and finishes at 922 °C. These values are in accordance with previous measurements on the same alloy for the heating rate involved [5,11]. Considering electrical resistivity measurements, a significant decrease of $R/R0$ is observed when the temperature reaches 834 °C. If this decrease is associated with the occurrence of phase transformation, the transformation starts at 834 °C and finishes at 938 °C. These values are respectively 16 °C lower and 16 °C higher than the beginning and ending transformation temperatures measured by dilatometry. Such differences in the transformation temperature measurements obtained by dilatometry and electrical resistivity were also reported by Fréchinet [5]. For the beginning of the transformation, they were mainly attributed to a delay in the macroscopic response of the length variations of the specimen [5]. In addition, one has also to consider that these differences may be associated with the dissolution of precipitates occurring previous to the $\alpha \rightarrow \beta$ transformation. The differences in the transformation temperature end may be associated with a higher dependence of the electrical resistivity on the chemical

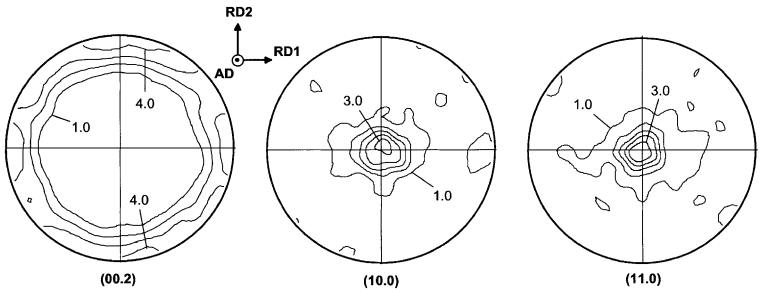

Fig. 3. (00.2), (10.0) and (11.0) pole figures of the α phase before transformation (contour lines are equally spaced of 1 unit in (00.2) pole figure and 0.5 in the others).

Table 2
Characteristic values of the α texture before and after transformation

	Min/max values of pole figures			Texture index	Max of the ODF	Kearn's factors		
	$(00.2)_\alpha$	$(10.0)_\alpha$	$(11.0)_\alpha$			F_{RD1}	F_{RD2}	F_{AD}
Starting α texture	0.0/4.4	0.5/3.3	0.5/3.7	2.5	6	0.478	0.433	0.09
Inherited α texture ($\sigma = 0$ MPa)	0.0/4.6	0.17/3.0	0.1/9.7	4.0	12	0.402	0.409	0.189
Inherited α texture ($\sigma = 8.2$ MPa)	0.0/3.7	0.3/2.4	0.2/6.2	2.4	9	0.420	0.348	0.232

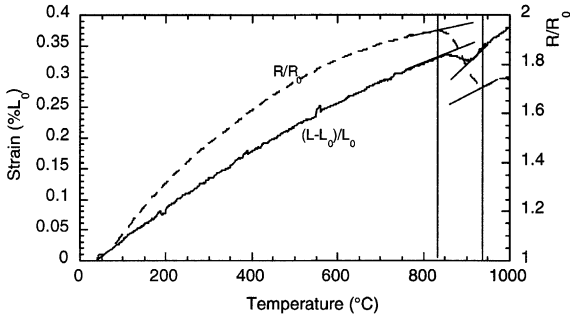

Fig. 4. Length and normalized electrical resistance variations measured during heating at 10 °C/s.

composition of the alloy, which is not homogeneous once the 'crystallographic' transformation is completed.

The dilatometric behavior reveals a small contraction (−0.03%) for the α → β transformation strain. The amplitude of this variation is largely dependent on the measurement direction because of the texture of the α phase and the anisotropic thermal behavior of the hcp structure. This effect has been verified on the tested material [14,15]. Here we only report the dilatometric curves corresponding to AD.

3.2.2. Inherited microstructure and texture

The microstructure of the α phase inherited after the β treatment shows a classical β-transformed microstructure (see Fig. 5). It is characterized by α plates (α_{GB})

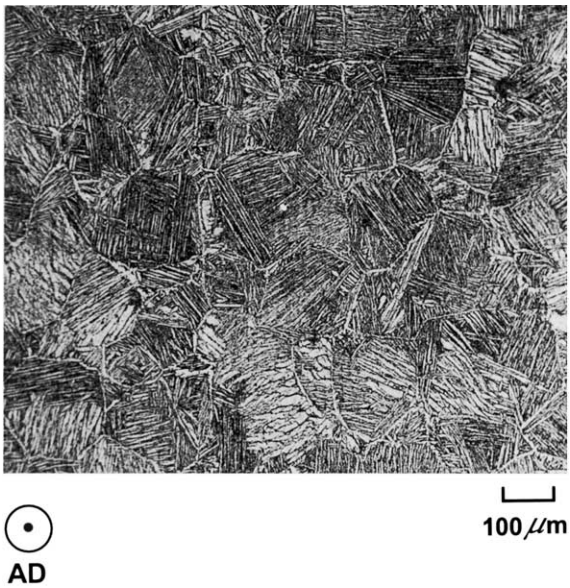

Fig. 5. Inherited α microstructure.

which preferentially nucleated at β/β grain boundaries, Widmanstätten α colonies which grew from the α_{GB} and finally α phase which nucleated within the β matrix.

The α_{GB} precipitation makes easy the observation of the equiaxe shape of the high temperature β grains whose size varies from 100 to 300 μm.

The analysis of the inherited orientations determined by EBSD confirms that the orientations of the α plates inherited inside each β grain are related to the β orientation by the Burgers relation. Each β grain can potentially give rise to 12 different α orientations. Nevertheless, in practice, only three to six different α orientations were identified in the visible section of the parent grains.

The inherited α texture without applied stress at heating is a sharp texture. The texture index is equal to 4 and the maximum value of the ODF is equal to 12 (see Table 2). This texture is characterized by a main ⟨11.0⟩//AD fiber ($\vec{c}$ axes in RD) and a minor fiber component corresponding to the orientations of α crystallites having their $\vec{c}$ axes at about 30° from the AD (see Fig. 6).

The comparison between the α texture before and after transformation makes clear that the $\alpha \rightarrow \beta \rightarrow \alpha$ transformation sequence, without applied stress at heating, has reinforced the texture sharpness. Moreover, the transformed texture only shows the ⟨11.0⟩//AD fiber, whereas the initial texture was formed by the ⟨uv.0⟩//AD fiber components (including the specific ⟨10.0⟩//AD and the ⟨11.0⟩//AD fibers).

3.3. Material behavior for transformation with applied stress

3.3.1. Length and electrical resistivity variations

The dilatometric curves for specimens transformed with an applied stress varying from 1.2 to 8.2 MPa during the heating part are shown in Fig. 7. As previously described, the tensile stress has only been applied into a direction parallel to AD, that means mainly parallel to the $\vec{a}$ axes of the α crystallites.

Fig. 7 clearly shows that, during the heating part, applied stress does not modify the behavior of the material until 860 °C. However, for all applied stresses, a dilatation is observed in the transformation temperature range while for 0 MPa we have a contraction (see Fig. 4). This change in mechanical behavior is mainly associated with the occurrence of transformation plasticity deformation [4,5,16]. Indeed, as we heat the alloy under stress, the length variations have different sources [3,8]: ε_{th} the expansion of the phases, ε_c the deformation associated with creep, and if phase change occurs, ε_{tr} the deformation associated with the phase change (a contraction on heating), and ε_{tp} the contribution of transformation plasticity.

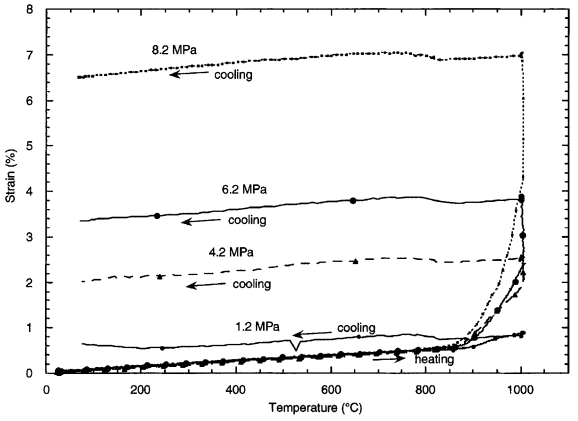

Fig. 7. Dilatometric curves for specimens transformed during heating under various applied stresses and cooling without stress.

For the stress of 1.2 MPa, the creep contribution is negligible. Indeed, once the $\alpha \rightarrow \beta$ transformation is completed, the dilatation coefficient of the β phase is the same as the one observed without applied stress. Moreover no noticeable creep is observed at 1000 °C. Thus one can consider that the additional deformation in the transformation temperature range is mainly associated with transformation plasticity. For stresses of 4.2–8.2 MPa, creep is clearly observed at 1000 °C. For 4.2 MPa, during heating, a change in the slope is observed at 955 °C; the deformation rate decreases. This

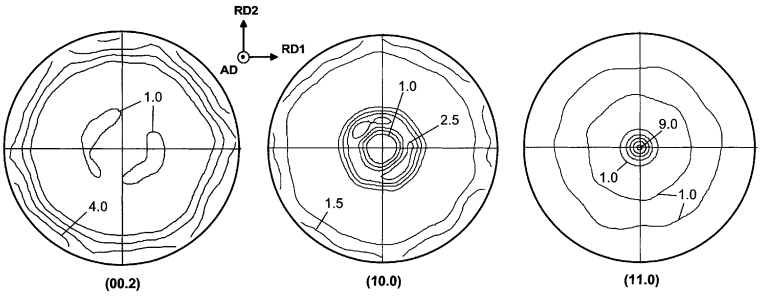

Fig. 6. (00.2), (10.0) and (11.0) poles figures of the inherited α phase (contour lines are equally spaced of 1 unit in (00.2) pole figure, of 0.5 units in (10.0) pole figure and of 2 units in (11.0) pole figure). Treatment without applied stress.

indicates at least that transformation plasticity is decreasing. For the applied stresses of 6.2 and 8.2 MPa, there is an increasing elongation associated with a large contribution of creep. The length variations are also measured during cooling. It is worth to recall that the stress was relieved. One observes that the dilatometric behavior is quite similar for all heating conditions.

A comparison of the dilatometric curve and the electrical resistivity variations obtained for the test performed under the stress of 8.2 MPa is given in Fig. 8. Considering the beginning of the transformation, it can be pointed out that the electrical variations deviate from the major curve in the temperature range of 810–830 °C. This temperature is 4–24 °C lower than the one without applied stress. Thus some stress/strain induced effect could be observed. From electrical resistivity measurements, the temperature at which transformation is completed could be estimated to 950 °C, temperature close to the one for no applied stress. Thus, considering that for all cases, transformation is completed at 950 °C, the deformation in the temperature range of the transformation can be estimated. The obtained values are reported in Fig. 9 versus the applied stress. If a linear variation of this deformation is assumed, the slope $d\varepsilon/d\sigma$ is equal to 1.6 GPa^{-1}.

The transformation plasticity deformation corresponds to a shear deformation component due to a favorable orientation of the transformed phase in the presence of an applied stress and a volume deformation component due to an anisotropic plastic accommodation of the transformation deformation. The contribution of each component to the observed deformation, can be quite different according to the material characteristics (microstructure, texture, sample shape) as well as to the treatment conditions (loading path, rate of temperature increase, atmosphere). In this work, all these parameters were held constant and it is not possible to discuss their influence on the deformation behavior of the material.

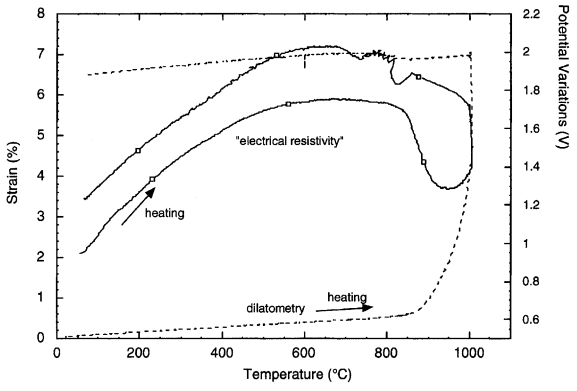

Fig. 8. Dilatometric and electrical variations during heating under 8.2 MPa and cooling without stress.

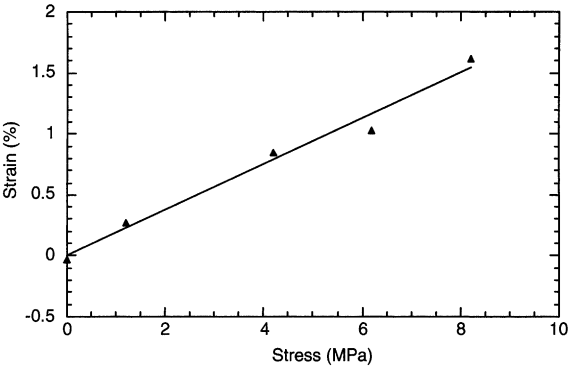

Fig. 9. Deformation in the temperature range of the $\alpha \rightarrow \beta$ transformation according to the applied stress.

Such a sensitivity of transformation plasticity deformation makes comparison with other published results rather difficult. Zwigl and Dunand report a value of 4.4 GPa^{-1} on zirconium for a complete transformation cycle $\alpha \rightarrow \beta \rightarrow \alpha$. For the single way, transformation on heating, they report a value of 2.3 GPa^{-1}. This value is close to the one obtained in this study for a Zy-4 rod. Our value can also be compared to that measured by Fréchinet (6.5 GPa^{-1}) on a Zy-4 cladding tube [5]. One observes that our value is four times lower than the one obtained by Fréchinet. This could be linked to the sensitivity of the transformation plasticity deformation to the sample shape. The deformation could be quite different if the sample section is of the order of magnitude of the size of the grains. This discrepancy can also be attributed to small texture differences between both samples.

3.3.2. Inherited microstructure and texture

The microstructure of the α phase, inherited after cooling from the β field, is not significantly modified by the applied stress at heating. It still corresponds to a classical β-transformed microstructure as described in the case where no stress is applied. Neither the high temperature β grain size nor the number of inherited colonies identified in each parent β grain seem significantly modified.

However, the texture of the inherited α phase (Fig. 10) exhibits some differences compared to the α texture obtained without applied stress (Fig. 6). Although the main components of the inherited α texture are the same as those observed without applied stress, the sharpness of the texture is significantly reduced. As indicated in Table 2, the maximum of the ODF has decreased from 12 (without applied stress) to 9 (with $\sigma = 8.2$ MPa), whereas the texture index has decreased from 4 to 2.4. This mainly corresponds to a decrease of orientation

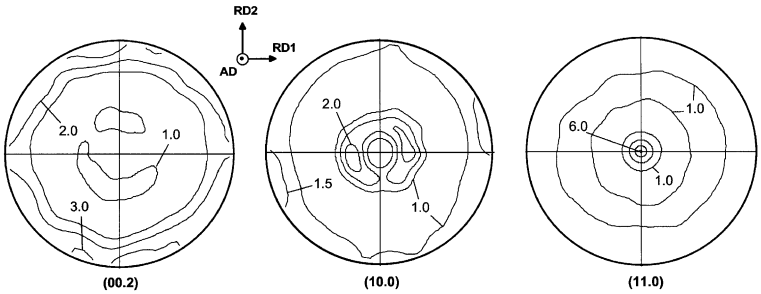

Fig. 10. (00.2), (10.0) and (11.0) pole figures of the inherited α phase (contour lines are equally spaced of 1 unit in (00.2) pole figure, of 0.5 units in (10.0) pole figure and of 2 units in (11.0) pole figure). Treatment with applied stress ($\sigma = 8.2$ MPa).

density around the ⟨11.0⟩//AD fiber as seen by the maximum values of the (11.0) pole figures (Figs. 6 and 10). The minor fiber component, corresponding to the orientations of α crystallites having their $\vec{c}$ axes at about 30° from the AD, has more or less the same intensity as without applied stress.

It can also be noticed that the inherited α texture is still sharper than the α texture before transformation, especially due to a reinforcement of orientation densities around the ⟨11.0⟩//AD fiber.

4. Discussion: influence of applied stress on the α → β → α texture change

The comparison of the α texture before and after transformation makes clear that for the investigated material, the α → β → α transformation sequence with or without applied stress at heating, has reinforced the texture sharpness. Moreover, with respect to the initial texture formed by the ⟨uv.0⟩//AD fiber components (including the specific ⟨10.0⟩//AD and the ⟨11.0⟩//AD fibers), the transformed textures only show the ⟨11.0⟩//AD fiber.

Such texture changes cannot be explained by a simple succession of transformations respecting the Burgers orientation relation (2). In fact, according to this relation, one initial α orientation can give rise to six β orientations, which each can transform into 12 α orientations.

$$\begin{aligned}&(1\,1\,0)_\beta//(00.2)_\alpha\\&[\bar{1}\,1\,\bar{1}]_\beta//[2\,\bar{1}.0]_\alpha.\end{aligned}\tag{2}$$

The orientation overlapping due to the α → β → α transformation would finally lead to 57 different α inherited orientations [17,18]. This set of orientations obviously includes the initial α orientation because each β orientation can potentially transform back into its parent α orientation. Consequently, a transformation without variant selection implies a large orientation multiplication as well as the holding of the initial α orientations, leading to smooth inherited textures. This is not observed for the investigated material. On the contrary, the number of inherited orientations is reduced and consequently the α textures sharper, whether stress is applied or not at heating.

To better understand the transformation mechanism leading to the observed texture changes, it is necessary to analyze the intermediate β textures. However, it is impossible to keep the β phase at room temperature, even after quenching. Thus, in this study, its texture has been evaluated from the inherited α texture thanks to restitution methods detailed in previous papers [19–21] and briefly described thereafter.

4.1. Intermediate β textures

The method used in this study consists in finding the ODF of the parent β phase by the deconvolution of relation (3), the ODF $f_\alpha(g)$ of the inherited α phase being known.

$$f_\alpha(g) = \int W(\Delta g) f_\beta\left(\Delta g^{-1} g\right) d\Delta g. \tag{3}$$

Eq. (3) expresses the relation between the parent f_β and the inherited f_α texture when no variant selection occurs during the β → α transformation. $W(\Delta g)$ is the orientation transformation function taking into account the Burgers orientation relation between lattices (2).

The search of $f_\beta(g)$ is performed so that its transformation into the ODF of the α phase is the closest to the measured inherited ODF $f_\alpha(g)$, keeping $f_\beta(g)$ positive. Practically, the calculation amounts to finding out the minimum of the quantity J_s:

$$J_s = \int \left[\int W(\Delta g) f_\beta\left(\Delta g^{-1} g\right) d\Delta g - f_\alpha(g) \right]^2 \mathrm{d}g \quad \text{with } f_\beta(g) \geqslant 0. \tag{4}$$

This method gives a good restitution of the parent texture, provided that no variant selection occurred in the

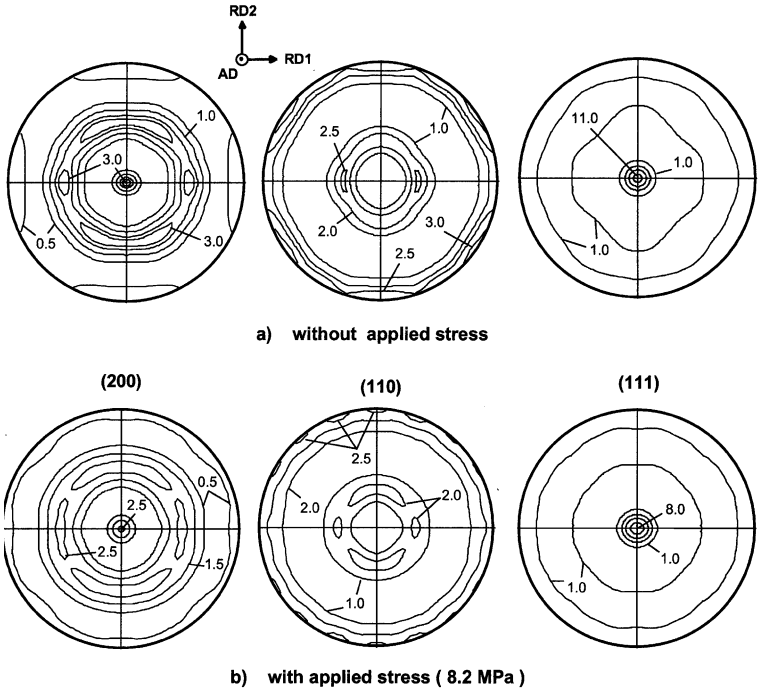

Fig. 11. (1 0 0), (1 1 0) and (1 1 1) calculated pole figures of the β phase (a) without applied stress at heating, (b) with applied stress ($\sigma =$ 8.2 MPa).

$\beta \rightarrow \alpha$ phase transformation. Up to now, even with the knowledge of variant selection, no author proposes a method able to accurately derive the parent β ODF from the global inherited ODF. In the case of variant selection, the individual orientation of the parent grains can be calculated by correlation of inherited orientations [19]. However, this requires local orientation determinations.

When the restitution method is applied in the case of variant selection, it gives the main trends of the real parent texture. Numerous simulations [20–22] have ascertained that, even if index J_s is not close to zero, the main orientations of the parent texture are always restituted by the calculation. Moreover, the deviation from zero of index J_s characterizes the importance of the variant selection in the $\beta \rightarrow \alpha$ phase transformation.

The restitution method applied to the α textures inherited with and without applied stress at heating gives the evaluation of the parent textures shown in Fig. 11. The corresponding index J_s and some characteristic values of the calculated β textures are detailed in Table 3.

4.2. Analysis of the texture modifications

First of all, it is interesting to notice the 'high value' of J_s ($J_s = 1.01$), especially when no stress is applied. This indicates that a strong variant selection occurred in the $\beta \rightarrow \alpha$ phase transformation when no stress is applied at heating. As a consequence, the calculated texture in Fig. 11(a), only gives the main trends of the real high temperature β texture.

In this case, the restitution method predicts a quite sharp β texture, mainly characterized by a $\langle 1\,1\,1\rangle//$DA fiber and a minor $\langle 1\,0\,0\rangle//$DA fiber (see Fig. 11(a)). The comparison of the $(1\,1\,0)_\beta$ and the $(00.2)_\alpha$ pole figures, gives some information about the $\beta \rightarrow \alpha$ variant selection. In fact, the Burgers orientation relation implies the

Table 3
Characteristic values of the calculated parent β textures

Calculated β texture	Index J_s	Min/max values of pole figures			Texture index
		$(1\,0\,0)_\beta$	$(1\,1\,0)_\beta$	$(1\,1\,1)_\beta$	
Without applied stress at heating	1.01	0.0/3.5	0.0/3.2	0.0/11.0	5.7
With applied stress ($\sigma = 8.2$ MPa) at heating	0.37	0.0/2.8	0.0/2.6	0.0/8.0	2.4

coincidence of all $\{1\,1\,0\}_\beta$ and $\{00.2\}_\alpha$ planes when no variant selection occurs. Therefore, the differences between the high temperature $(1\,1\,0)_\beta$ and the inherited $(00.2)_\alpha$ pole figures allow one to identify the variants being preferentially selected during the $\beta \rightarrow \alpha$ transformation. From Figs. 6 and 11(a), it appears that the variants inherited from β orientations having the $\{1\,1\,0\}_\beta$ plane normal tilted to 30° from the AD are less numerous than expected. On the contrary, the α variants belonging to the $\langle 11.0\rangle//$AD fiber (inherited from β orientations having the $\{1\,1\,0\}_\beta$ plane normal tilted of 90° from the AD) are favored.

It is also interesting to notice that this variant selection is reduced when a stress up to 8.2 MPa is applied (see the value of J_s in Table 3). This is probably linked to the metallurgical state of the high temperature β phase, inherited from the $\alpha \rightarrow \beta$ transformation under stress. Additionally, the creep deformation of the β phase, pointed out on the dilatometric curves, could also have changed the metallurgical state of the β phase. In particular, it can be assumed that the resulting local stress field in the β phase is so that the nucleation rate of any other variants, belonging not obviously to the $\langle 11.0\rangle//$AD fiber, is increased. In the case of titanium alloys, previous studies pointed out that the plastic deformation of the parent phase increases the nucleation rate of the α phase as well as the number of inherited colonies [23]. In any case, this reduction in variant selection explains the decrease of orientation densities around the $\langle 11.0\rangle//$DA fiber, in the inherited α texture when stress is applied at heating.

The effect of applied stresses on the β texture is difficult to analyze in details because the calculated β textures only indicate the main trends of the real β textures. Moreover, the calculated β textures with and without applied stress only differ by the relative density of each fiber (see Fig. 11). However, the restitution method does not predict a noticeable sharper texture when stress is applied at heating. In the future, texture analysis of the β phase at high temperature are planed using neutron facilities. Applying a stress at heating induces transformation plasticity as derived from the dilatometric curves and does not increase the sharpness of the β texture. Thus the contribution of a preferential orientation of the β phase to the transformation plasticity deformation cannot be pointed out, even qualitatively.

5. Conclusion

This contribution reports some effects of an axial stress applied during the $\alpha \rightarrow \beta$ transformation of Zy-4, on the $\alpha \rightarrow \beta \rightarrow \alpha$ phase transformation as well as on the inherited microstructures and textures. The thermomechanical dilatometric tests clearly pointed out the existence of transformation-induced plasticity when the $\alpha \rightarrow \beta$ transformation occurred under stress. This transformation-induced plasticity effect has been observed for stresses of 1.2 to 8.2 MPa. Beyond 4.2 MPa, creep has been identified. The observed mechanical behavior of the material is in good agreement with results published previously.

The analysis of the material after the $\alpha \rightarrow \beta \rightarrow \alpha$ transformation sequence reveals a strong influence of applied stresses, on the inherited α textures. In the case of a shear transformation, it is generally observed that applying a stress during the transformation, favors some crystallographic orientations of the transformed product and consequently sharpens its texture. However, in this study, this fact has not been observed: as the applied stress increased, the inherited α textures became significantly smoother and remained characterized by the same texture components.

A detailed analysis of the texture modifications induced by the β treatment without applied stress reveals a strong variant selection, especially in the $\beta \rightarrow \alpha$ transformation at cooling (the $\alpha \rightarrow \beta$ one at heating has not been extensively studied). The intensity of the $\beta \rightarrow \alpha$ variant selection decreases significantly when stress is applied at heating. This effect is to relate to the metallurgical state of the β phase inherited from the $\alpha \rightarrow \beta$ transformation under stress along with β phase creep. It can be assumed that the resulting local stress field in the β phase is such as all variants in the transformation at cooling, have the same nucleation potential. The understanding of the involved mechanisms will require some additional efforts, notably the study of the correlation between the nucleation/growth mechanism and the associated variant selection rules.

Acknowledgements

We acknowledge the CEZUS Company, and in particular Dr Pierre Barberis Research Engineer, for supplying the Zy-4 rod and J.C. Brachet (CEA/SRMA) for fruitful discussion.

References

[1] C. Lemaignan, A.T. Motta, in: R.W. Cahn, et al. (Eds.), Materials Science and Technology, VCH, 1994, p. 1.
[2] F.J. Erbacher, S. Leistikow, in: R.B. Adamson, L.F.P. Van Swam (Eds.), Zirconium in the Nuclear Industry: 7th International Symposium, ASTM STP, 939, American Society for Testing Materials, Philadelphia, PA, 1987, p. 451.
[3] G.W. Greenwood, R.H. Johnson, Proc. Roy Soc. London 283 A (1965) 403.
[4] P. Zwigl, D.C. Dunand, Metall. Mater. Trans. A 29 (1998) 2571.

[5] S. Fréchinet, thesis, Ecole des Mines de Paris, 2001.
[6] F. Abrassart, thesis, Ecole des Mines de Nancy, 1972.
[7] E. Gautier, J.S. Zhang, X.M. Zhang, J. Phys. IV 5 (1995) 41 (C8, sup. au J. Phys. III).
[8] C.L. Magee, thesis, Carnegie Mellon University, 1966.
[9] J.B. Leblond, J. Devaux, J.C. Devaux, Int. J. Plast. 5 (1989) 551.
[10] F.D. Fisher, Acta Metall. Mater. 38 (1990) 1535.
[11] H.J. Bunge, Texture Analysis in Materials Science, Cuvillier, Göttingen, 1993.
[12] S. Matthies, F. Wagner, Phys. Status Solidi B K11 (1996) 196.
[13] J.L. Béchade, private communication.
[14] J.C. Brachet, J.L. Béchade, A. Castaing, L. Le Bland, T. Jouen, Mater. Sci. Forum 273–275 (1998) 529.
[15] A. Cerqueira, rapport de stage, Novembre 2000.
[16] D. Leriche, E. Gautier, A. Simon, in: 6th World Conference on Titanium, France, 1988, p. 163.
[17] W.G. Burgers, Physica 1 (1934) 561.
[18] G. Braichotte, thesis, Université Paris 11 Orsay, 1974.
[19] M. Humbert, H. Moustahfid, F. Wagner, C. Esling, Scripta Met. Mater. 30 (1994) 377.
[20] M. Humbert, N. Gey, J. Appl. Crystallogr. 32 (1999) 21.
[21] M. Humbert, N. Gey, C. Esling, J. Appl. Crystallogr. 33 (2000) 206.
[22] M. Humbert, N. Gey, B. Gardiola, C. Esling, Acta Mater. 49 (2001) 445.
[23] E. Laude, E. Gautier, D. Delannoy, P. Archambault, in: Proceedings of the 9th World Conference on Titanium, 1999, p. 149.